Rock and Soil Mechanics 2026 47(2): 627–639 ISSN 1000–7598
https: //doi.org/10.26599/RSM.2025.94300112 journal homepage: rocksoilmech.whrsm.ac.cn

Deterioration characteristics of mechanical properties of heterogeneous accumulation of iron tailings sand under the action of freeze-thaw cycles

ZHANG Hong-yue, JIN Jia-xu, WU Peng-fei

School of Civil Engineering, Liaoning Technical University, Fuxin, Liaoning 123000, China

Abstract: The heterogeneous accumulation structure of tailings sand poses a serious threat to the safe and stable operation of tailings ponds. However, analyses of how freeze-thaw cycles affect the mechanical properties of heterogeneous tailings-sand accumulations are limited. In this paper, based on triaxial compression tests and nuclear magnetic resonance tests, we analyze the macroscopic mechanical properties and mesoscopic pore evolution of the heterogeneous accumulation structure of tailings sand under the action of freeze-thaw cycles. Results show that as the number of freeze-thaw cycles rises, the shear strength of specimens with different interface inclination angles decreases significantly, and the magnitude of decrease correlates positively with the inclination angle. Under low confining pressure, the stress-strain curves of specimens with larger inclination angles exhibit strain softening. Under the action of freeze-thaw cycles, the deformation modes of coarse sand, fine sand, and specimens at various inclination angles can be categorized as shear dilation or a combination of shear dilation and contraction, with the failure mode being transverse fracture. Freeze-thaw cycles cause the "migration and accumulation" of pore water in tailings sand specimens. Interface structures of tailings sand accumulations with different particle sizes can significantly shorten the "migration and accumulation" period, presenting more intense phenomena of small pore connectivity and large pore collapse. Confining pressure strengthens tailings sand and can amplify freeze-thaw–induced strength deterioration. The filling of the lower-layer pore spaces by fine particles increases the interfacial strength of the tailings-sand at the interface. The small particles located above the interface act as weak structural planes and are more prone to deterioration. These findings provide both macroscopic and microscopic perspectives on how freeze-thaw cycles degrade the mechanical properties of sand and soil.

Keywords: freeze-thaw cycles; heterogeneous; iron tailings sand; macro-mesoscopic combination; mechanical properties

1 Introduction

The tailings pond is a man-made hazard source of debris flow that has high potential energy. For several years or even more than a decade, various natural factors such as rainfall, earthquakes, freeze-thaw and other unfavorable factors constantly or periodically threaten its safety. Once the tailings pond is destabilized and damaged, it will cause irreversible consequences to the people, economy and environment in the downstream areas[1-5].

As per the statistical data provided by Yin et al.[6], there are over 12 000 tailings ponds in China. Nearly 95% of tailings ponds adopt the upstream dam construction method. And nearly 85% of these tailings ponds are situated in cold regions[7]. Existing studies have shown that under the action of infiltrating water and evaporation, the phreatic line in the tailings pond will experience a short-term rise. During the accumulation process of tailings sand, hydraulic sorting will also lead to loose tailings structure and a high phreatic line level. Therefore, tailings ponds located in seasonally frozen regions will be affected by freeze-thaw action, resulting in serious expansion and subsidence in the reservoir area[8-10]. Based on this, scholars in the industry have carried out a large number of studies on the strength degradation of tailings sand under the impact of freeze-thaw cycles from a macroscopic perspective. Yang et al.[11] carried out uniaxial compression tests on four kinds of frozen tailings sand and elaborated in detail the variation laws of compressive strength and deformation modulus of frozen tailings sand under various factors. Wei et al.[12] conducted triaxial shear tests on ultrafine particle tailings that had undergone freeze-thaw cycles, proving that freeze-thaw cycles have a significant weakening impact on the shear strength of tailings materials. Liu et al.[10] studied the impact of freeze- thaw cycles on the cyclic dynamics of tailings sand through undrained cyclic triaxial tests. He found that freeze-thaw cycles have a significant impact on the cyclic dynamic response of tailings sand. Moreover, with the increase in freeze-thaw cycles, the cyclic resistance to failure becomes smaller and the failure pore water pressure becomes larger. Liu et al.[7] explored the mechanical and deformation characteristics of tailings sand under the impact of freeze-thaw cycles. The results indicate that cementation damage and internal pore expansion of tailings are the main factors affecting the mechanics and deformation of tailings sand. Li et al.[13] studied the mechanical properties and structural variations of tailings sand under different numbers of freeze-thaw cycles, confining pressures, and moisture contents. The test conclusion is that with the increase in freeze-

Received: 17 March 2025 Accepted: 30 May 2025
This work was supported by the General Program of National Natural Science Foundation of China (51974145).
First author: ZHANG Hong-yue, male, born in 1997, PhD, Lecturer, research interests: rock and soil mechanics and engineering.
E-mail: lgd1232020@163.com
Corresponding author: JIN Jia-xu, male, born in 1984, PhD, Professor, research interests: resource utilization of solid waste. E-mail: jjx_605@163.com

thaw cycles, the shear strength of tailings sand decreases, and the pore structure of tailings sand undergoes irreversible deformation after 40 freeze-thaw cycles. Thus, the pore distribution and mechanical properties of tailings sand following freeze-thaw cycles are extremely significant for the safe and stable operation of tailings ponds in seasonally frozen areas.

The research on the impact of heterogeneous structures on the stability of artificial structures has emerged long ago[14-15]. Due to the wet discharge method adopted in tailings ponds, after being sorted by hydraulic forces, the tailings will also be unevenly distributed within the pond area, manifesting characteristics such as accumulated interlayers and interlayer lenticular bodies, as shown in Fig. 1. Some scholars have conducted research on the lenticular body phenomenon existing in tailings ponds. Zhang et al.[16] studied the layered structure of tailings sand by combining macro and micro methods, and clarified the mechanical degradation characteristics of the layered structure and the corresponding micromechancial mechanism. Chen et al.[2] conducted research on the strength and deformation characteristics of tailings sand with fine-grained interlayers based on Coulomb's theory. The results indicate that when the inclination angle of the interlayer is close to 60°, the fine-grained interlayer controls the strength and deformation of the tailings sand specimen. Tian et al.[17] explored the problem of differences in particle size in different areas of the tailings pond. Zhang et al.[18] analyzed the types of lenticular bodies of multiple tailings dams in summer and winter in China, discussed the causes of lenticular bodies, established a triaxial model with flexible boundaries, and analyzed the influence of different lenticular bodies on the mechanical properties of tailings. Thus, it can be seen that the lenticular bodies and layered structures existing in the reservoir area greatly affect the strength of tailings sand, which in turn leads to instability and deformation of the tailings pond.

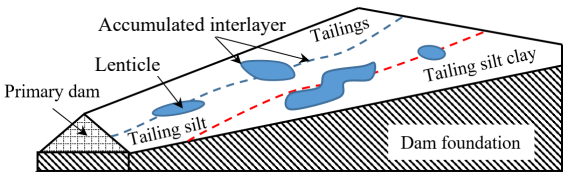


Fig. 1 Distribution of accumulated interlayers and lenticles in tailings reservoir

Although considerable progress has been made in the study on the macroscopic mechanical properties of tailings sand containing lenticular bodies, the strength weakening law of the heterogeneous accumulation of tailings sand after experiencing periodic freeze-thaw cycles is still unclear. Moreover, there are relatively few studies on quantitatively analyzing the impact of freeze-thaw cycles on the physical characteristics of the heterogeneous structure of tailings sand from a microscopic perspective. Therefore, it is necessary to explore the macroscopic mechanical properties and microscopic pore evolution mechanism of the heterogeneous structure of tailings sand under the impact of freeze-thaw cycles. From a combined macro and micro perspective, the deterioration mechanism of the heterogeneous accumulation of tailings sand under the freeze-thaw effect should be ascertained.

2 Experimental materials

The sampling site of tailings sand is located in Tongnai Iron Mine, Fuxin Mongolian Autonomous County, Fuxin City, Liaoning Province, China. The annual average precipitation is between 420 and 540 mm. The tailings sand samples were collected at the surface layer (0−15 cm) of the dry beach of the tailings pond and then carefully transported to the laboratory. The basic physical parameters of tailings sand were measured by the pycnometer method, sieving method and cone liquid limit instrument. The results are listed in Fig. 2 and Table 1. Chemical composition analysis: the content of CaO in iron tailings sand is 7.31%, the content of SiO_2 is 47.56%, the content of Al_2O_3 is 7.12%, the content of Fe_2O_3 is 24.65%, the content of MgO is 5.42%, and the remaining oxides account for 7.94%. According to the *Code for design of tailings facilities* (GB 50863−2013)[19], this iron tailings sand belongs to fine tailings sand.

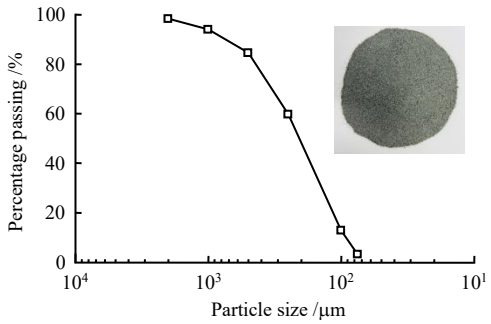


Fig. 2 Particle gradation curve of iron tailings sand

Table 1 Physical parameters of iron tailings sand

Specific gravity G_s	Moisture content /%	Void ratio e	Dry density /(g • cm^{-3})	Plastic limit /%	Liquid limit /%	Plasticity index
2.67	14.87	0.58	1.69	10.6	17.5	6.9

3 Macroscopic mechanical characteristics of the heterogeneous structure of tailings sand under freeze-thaw cycles

3.1 Specimen preparation and freeze-thaw

The tailings sand taken from the dry beach of the tailings pond is dried and sieved to obtain two particle size ranges of tailings sand: 0.25−2 mm (coarse sand, abbreviated as C) and <0.25 mm (fine sand,

abbreviated as F). The sieved C and F tailings sands are made into a moisture content of 15% and then put into sealed bags and moistened for standby. The material of the triaxial test specimen tube for tailings sand is plexiglass tube with an inner diameter of 39.1 mm, a height of 80 mm and a wall thickness of 3 mm. Specimens with interface inclination angles of 30°, 45°, and 60° are compacted by a customized compaction rod. Specimens of C, F, and 0° inclination angles are compacted by a compaction hammer. During the sand filling process, a fine brush is used to evenly brush the tailings sand on the surface of the inclined plane. The completed specimens are sealed in plastic wrap and stored in a refrigerator. The test plan and finished specimens are listed in Table 2. The temperature range of freeze-thaw cycles is set at −20 ℃ to 20 ℃. The triaxial instrument model is GDS DYNTTS frozen soil triaxial instrument. Unconsolidated undrained triaxial shear test (UU) is adopted. The confining pressure is set at 100, 200, and 300 kPa. The shear rate is set at 1%/min. Loading is stopped when the axial strain reaches 15%.

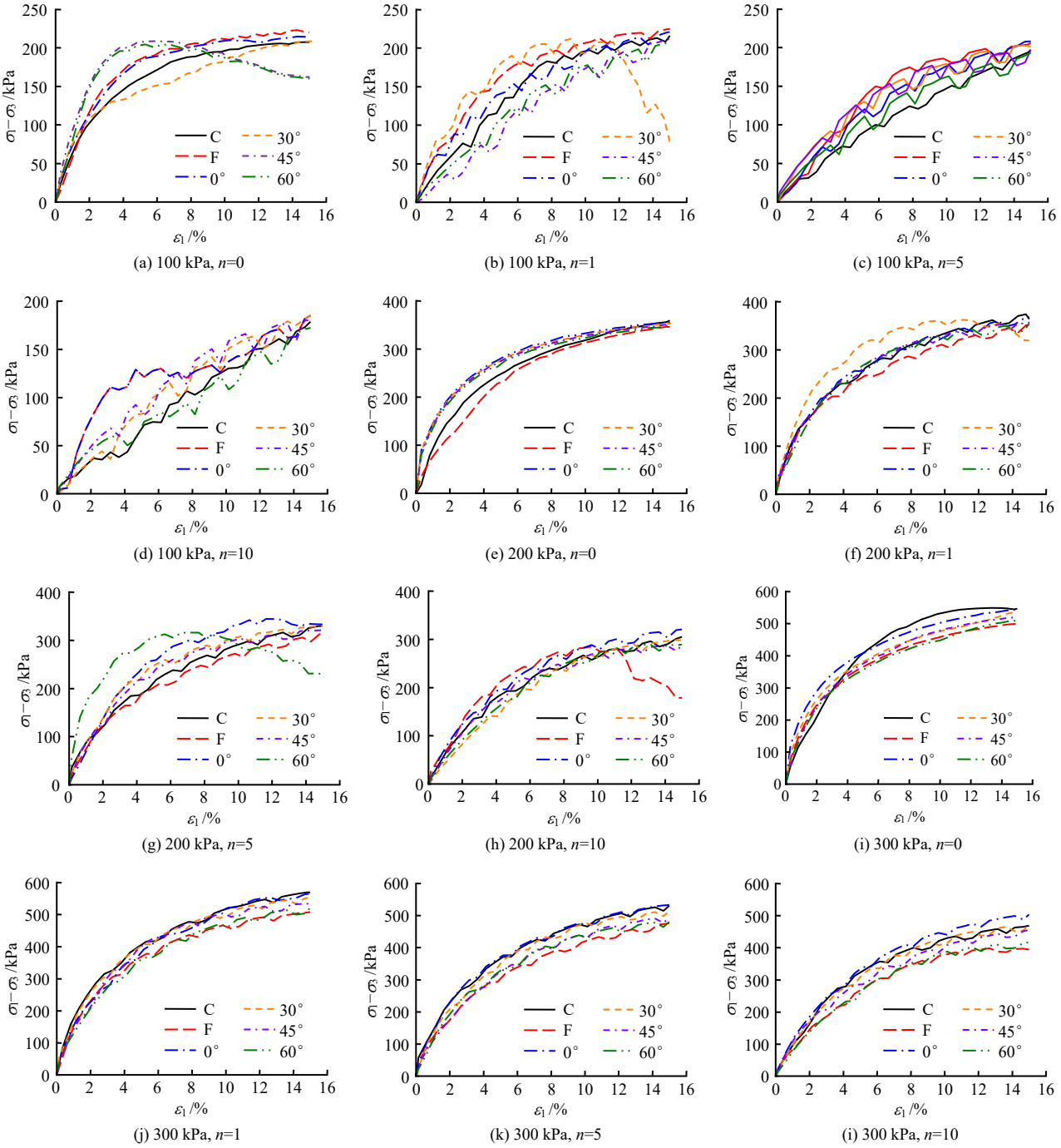
Table 2 Test plan

Particle size interval /mm	0.25−2	<0.25	0.25−2, <0.25			
Moisture content /%	15	15	15			
Freeze-thaw cycles	0, 1, 5, 10	0, 1, 5, 10	0, 1, 5, 10			
Interface inclination angle /(°)	—	—	0	30	45	60
Specimen photos						

3.2 Triaxial test results

3.2.1 Stress-strain curve

As illustrated in Fig. 3, which is the stress-strain curves of specimens with different inclination angles under the action of number of freeze-thaw cycles. It can be observed that most of the remaining curves are of strain hardening type. And with the increase in number of freeze-thaw cycles, they decrease to different degrees. Before unfreezing and thawing, the deviator stress- strain curves of each specimen are relatively smooth. After experiencing freeze-thaw cycles, the curves show the characteristics of stage depression. After one freeze-thaw cycle of the specimen with a 0° inclina- tion angle, the stress-strain curve is rather tortuous. After five number of freeze-thaw cycles, the stress-strain curve under a confining pressure of 200 kPa transitions from strain hardening to strain softening. After ten freeze- thaw cycles, it returns to strain hardening. Before the specimen with a 30° inclination angle experiences freeze-thawing, the curve is of strain hardening type. After one freeze-thaw cycle, the curves under confining pressures of 100 kPa and 200 kPa turn to strain softening, and the deviator stress is lower than that of the unfrozen specimen. After five number of freeze-thaw cycles, the stress-strain curve becomes a strain hardening type, and both the curve slope and the peak deviator stress gradually increase. For specimens with interface inclination angles of 45° and 60°, before freezing, the stress-strain curves under a confining pressure of 100 kPa are of strain softening type. After experiencing freeze-thaw cycles, the stress-strain curves all show strain hardening. After five number of freeze-thaw cycles of the specimen with a 60° inclination angle, softening occurs under a confining pressure of 200 kPa. Strain softening of specimens with interface inclination angles mostly occurs under low confining pressures. The impact mechanism of various inclination angles on the stress-strain curve of specimens is manifested as follows: After the initial freeze-thaw time, due to the increase in volume caused by the freezing of pore water at the accumulation interface of different particle sizes of tailings sand in the specimen, the small particles in the upper layer fill the pores in the lower layer. The pores decrease, the particle arrangement becomes compact, and the capillary action is enhanced. Therefore, the peak value of the stress-strain curve of the specimen with interface inclination angle first increases. However, with the increase in number of freeze-thaw cycles, the migration of pore water is completed, the volume expansion of large pores reaches the maximum value, and the filling of the accumulation interface of different particle sizes is completed. The pores are relatively small, and it is difficult for the small particles in the upper layer to continue filling the large particles in the lower layer through the interface. Therefore, the peak value of the stress-strain curve of the specimen decreases.



(a) 100 kPa, n=0 (b) 100 kPa, n=1 (c) 100 kPa, n=5

(d) 100 kPa, n=10 (e) 200 kPa, n=0 (f) 200 kPa, n=1

(g) 200 kPa, n=5 (h) 200 kPa, n=10 (i) 300 kPa, n=0

(j) 300 kPa, n=1 (k) 300 kPa, n=5 (i) 300 kPa, n=10

Fig. 3 Stress-strain curves of specimens with different inclination angles under freeze-thaw cycles

3.2.2 Shear strength

The shear strength of specimens with various inclination angles under the action of number of freeze-thaw cycles is illustrated in Fig. 4. With the increase in number of freeze-thaw cycles, the shear strength of specimens with various inclination angles shows a trend of increasing first and then decreasing. And under confining pressures of 200 kPa and 300 kPa, the strength degradation of tailings sand is more significant. With the increase of the interface dip angle, the increase in the shear strength of tailings sand specimens due to the initial freeze-thaw time gradually decreases, and after 10 freeze-thaw cycles, the degree of strength degradation gradually increases. Under various number of freeze-thaw cycles, the strength of tailings sand with four inclination angles is shown as: 0°>30°>45°> 60°. The greater the confining pressure, the more obvious the difference in shear strength between various inclination angles. Under the conditions of 0 and 1 freeze-thaw cycles with a confining pressure of 100 kPa, the shear strength of the specimen with a 0° inclination angle is between that of the C and F specimens. With the increase in number of freeze-thaw cycles, the strength of the 0° specimen exceeds that of the F specimens. The shear strength of specimens with inclination angles of 30° and 45° is between that of the C and F specimens. Under confining pressures of 200 kPa and 300 kPa, when the number of freeze-thaw cycles are 0 and 1, the strength of specimens with different inclination angles is between that of the C

and F specimens. When the number of freeze-thaw cycles is 5, the shear strength of the specimen with a 0° inclination angle exceeds that of the C specimen. In addition, it can also be remarked that the influence of freeze-thaw cycles on the shear strength of tailings sand is associated with the confining pressure. That is, as the confining pressure increases, the degree of strength degradation of tailings sand increases, and the difference in shear strength of tailings sand with various inclination angles increases. This can be explained as follows: When the confining pressure is relatively low, the torsion, friction, and occlusion between tailings sand particles are weakly affected by the confining pressure. Therefore, the difference in shear strength between tailings sands of various particle sizes is relatively low. When the confining pressure increases, it has a strengthening impact on tailings sand and can magnify the influence of number of freeze-thaw cycles on the strength degradation of tailings sand, the confining pressure has a strengthening effect on tailings sand, which can amplify the influence of freeze-thaw cycles on the strength degradation of tailings sand. The force chain between tailings sand particles is more easily broken, leading to the rearrangement and combination of particles.

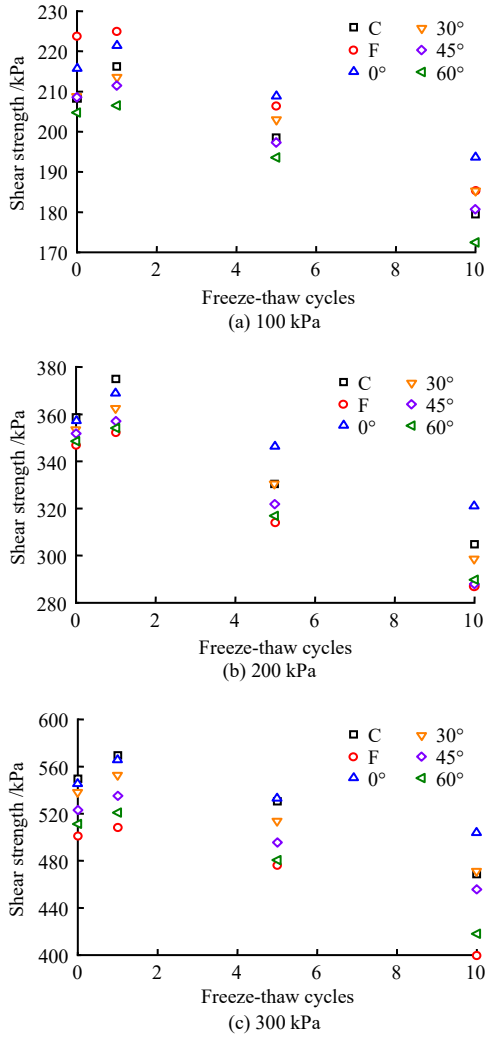


Fig. 4 Shear strength of specimens with different inclination angles under freeze-thaw cycles

3.2.3 Shear strength parameters

Based on Coulomb's law and combined with the triaxial test results of tailings sand specimens, stress circles and failure envelopes are drawn to obtain the shear strength parameters c and φ of specimens with various inclination angles under the impact of freeze-thaw cycles, as illustrated in Fig. 5. From the Fig. 5, with the increase in number of freeze-thaw cycles, the cohesion of specimens with various interface inclination angles gradually decreases, and the internal friction angle first increases and then decreases. As the inclination angle of the interface increases, the relationship of cohesion of each specimen is: 60°> 45°>0°>30°, and the relationship of internal friction angle is: 0°>30°> 45°>60°. After 10 freeze-thaw cycles, the cohesion of tailings sand with interface inclination angles of 0°, 30°, 45°, and 60° is reduced by 31.96%, 12.23%, 28.82%, and 14.42% respectively compared with that before freezing and thawing, and the internal friction angle is reduced by 4.67%, 7.98%, 8.51%, and 11.34% respectively compared with that before freezing and thawing. That is, with the increase in inclination angle of the interface increases, the greater the influence of freeze-thaw on tailings sand, and the more obvious the strength degradation effect. The variation law of cohesion with the inclination angle of the interface discovered in this paper is consistent with the variation law of cohesion with the interface angle observed by Zhao et al.[20]. In addition, after the initial freeze-thaw time, the cohesion of tailings sand with various inclination angles may increase slightly or decrease,

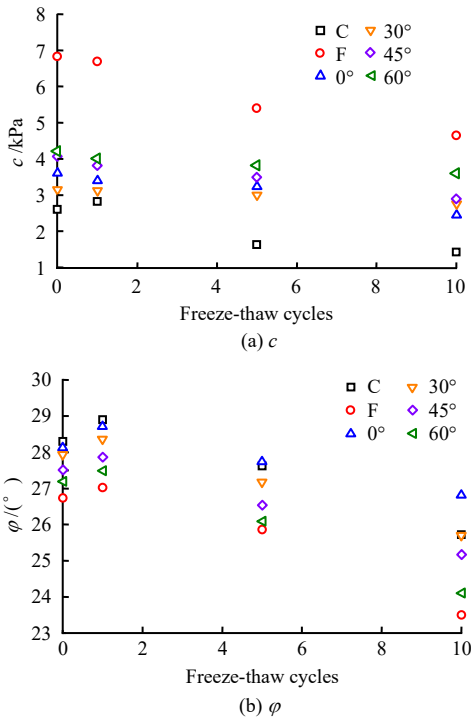


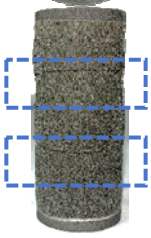
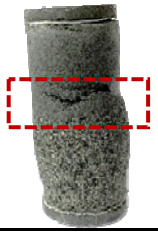
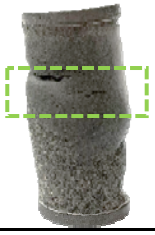
Fig. 5 Cohesion and internal friction angle of specimens with different inclination angles under freeze-thaw cycles

while the internal friction angle increases significantly. Thus, the strengthening impact of the initial freeze-thaw on the shear strength of tailings sand can be attributed to the increase in the internal friction angle. The increase in the internal friction angle will effectively increase the intergranular occlusion and sliding friction. And after the first freeze-thaw, the pore water is redistributed. The capillary action generates positive pressure between the tailings sand particles. This positive pressure generates frictional strength between the particles. Macroscopically, it is manifested as “false cohesion”. The increase in the internal friction angle also leads to an increase in “false cohesion”.

3.2.4 Failure mode

Table 3 shows the failure modes of specimens with various inclination angles under various numbers of freeze-thaw cycles and a confining pressure of 200 kPa. With the increase in number of freeze-thaw cycles, the axial strain of specimens with various inclination angles shows an increasing trend. And with the increase in inclination angle, the crack development of each specimen becomes more intense. Before freezing and thawing of specimens with inclination angles of 0°, 30°, and 45°, the shear failure is not obvious and the axial deformation is small. After one freeze-thaw cycle, the small particles in the upper layer and the large particles in the lower layer of the specimen show dilatancy characteristics, while shrinkage occurs at the interface of the accumulation layer. After five freeze-thaw cycles, at the interface of specimens with inclination angles of 0° and 30°, there is dilatancy, and the top and bottom of the specimen are contracted. At the same time, primary cracks begin to appear on the surface of the specimen. For the specimen with an inclination angle of 45°, after five freeze-thaw cycles, it is consistent with the initial freeze-thaw, still showing dilatancy characteristics of small particles in the upper layer and large particles in the lower layer, and shrinkage at the interface. After 10 freeze-thaw cycles, the primary cracks on the surface of specimens with inclination angles of 0° and 30° further develop, and secondary cracks are generated. While the primary cracks of the specimen with an inclination angle of 45° stop developing. And with the increase in axial load, the crack voids are compacted, and the dilatancy of small particles in the upper layer and large particles in the lower layer of the specimen is intensified. Before freezing, the specimen with an inclination angle of 60° shows significant dilatancy characteristics. The expansion area is at the interface between the coarse sand layer and the interface. After one freeze-thaw time, the dilatancy characteristics of the specimen do not further intensify, but primary cracks appear at the interface between the fine sand layer and the interface. After five freeze-thaw cycles, the primary

Table 3 Failure modes of specimens with different inclination angles under different freeze-thaw cycles

Freeze-thaw cycles	C	F	0°	30°	45°	60°
0						
1						
5						
10						

cracks develop laterally and almost penetrate the fine sand layer. After 10 freeze-thaw cycles, the primary cracks stop growing, secondary cracks begin to appear and develop, and secondary cracks are generated at the interface between the coarse sand layer and the interface. The dilatancy characteristics at the interface between the fine sand layer and the interface are obvious.

Under the action of freeze-thaw cycles, the deformation modes of C, F, and specimens with various inclination angles can be summarized as: dilatancy, coexistence of dilatancy and contraction, and the failure mode is transverse fracture. (1) Dilatancy: A common shear deformation mode of sandy soil. The characteristic is that the specimen expands from the middle to the outside during the shearing process. The shear deformation mode of C tailings sand is dilatancy. (2) Coexistence of dilatancy and contraction: There are local expansion and contraction phenomena in the specimen during the shearing process, and the two are alternately distributed along the longitudinal direction. The shear deformation mode of F tailings sand and tailings sand with various inclination angles is the coexistence of shearing and contraction. (3) Transverse fracture: Primary cracks are generated at the interface between dilatancy and contraction and grow laterally. Under the action of freeze-thaw, the failure modes of F and specimens with various inclination angles are all transverse fractures.

4 Evolution of pore structure of heterogeneous structure of tailings sand under freeze-thaw cycles

4.1 Nuclear magnetic resonance test

The preparation process of nuclear magnetic resonance specimens is the same as that of triaxial specimens. The material of the specimen tube is quartz glass with an inner diameter of 32mm, a height of 60mm and a wall thickness of 3mm. The moisture content of the prepared C, F, and specimens with various inclination angles is all 15%. The number of freeze-thaw cycles is set to 0, 1, 5, and 10, and the inclination angle of the accumulated interface is set to 0°, 45°, and 60°. The model of the nuclear magnetic resonance instrument used is MesoMR12-060H-I. The magnetic field strength is 0.3 T±0.03 T/0.5 T±0.03 T. The magnetic field uniformity is $\leqslant 3\times10^{-5}$. The maximum sample detection range is a cylinder with ϕ38mm×H100 mm. The sample injection direction is longitudinal. The magnet shape is a closed square shape. The pulse sequence is Carr-Purcell-Meiboom-Gill (CPMG). The magnetic field strength is 12 MHz. The waiting time is 4 500 ms. The echo time is 0.1 ms. The number of accumulations is 32. The magnet temperature is 20 ℃. The immersion saturation method specified in the *Standard for geotechnical test method* (GB/T 50123−2019)[21] was used to saturate the iron tailings sand specimens.

According to the relationship between relaxation time and pore size[22-23]:

$$\frac{1}{T_2}=\rho_2\frac{S}{V} \tag{1}$$

where T_2 is the transverse relaxation time (ms); ρ_2 is the surface relaxation coefficient (μm/ms); and S and V are the pore surface area (μm^2) and volume (μm^3) respectively.

When assuming that the pores of tailings sand are spherical, the above formula can be simplified as

$$\frac{1}{T_2}\approx\rho_2\frac{6}{D} \tag{2}$$

where D is the pore diameter.

4.2 Nuclear magnetic resonance test results

4.2.1 Pore distribution

Li et al.[24] put forward a method to obtain the pore ratio of specimens through NMR tests. According to the total area of the known initial sample T_2 relaxation time distribution curve and the pore ratio, the pore ratios of other specimens under different conditions are calculated, and the accuracy of this method is verified. Therefore, this paper uses this method to convert the amplitude on the ordinate of the specimen T_2 spectrum into porosity, and convert the abscissa relaxation time into pore diameter D through Eq. (2). Based on the study of Fan et al.[25], Wang et al.[26] and others, combined with the nuclear magnetic resonance test results of tailings sand, the pores are divided into micropores (<2 μm), mesopores (2−15 μm), macropores (15 −2 000 μm), fissures (>2 000 μm).

As illustrated in Fig. 6, the pore characteristics of specimens with various inclination angles change significantly, and the pore size distribution in each interval fluctuates strongly. After one freeze-thaw time, the porosity of the C specimen changes little, while the porosity of the F specimen and specimens with inclination angles of 0°, 45°, and 60° increases significantly, indicating that the F tailings sand shows freezing characteristics earlier than the C tailings sand. This is because the particle size of the F tailings sand is smaller and the shape is more regular, and most of the pore water is in the form of free water, so it freezes earlier than the C tailings sand. After five freeze-thaw cycles, the porosity of the C and F specimens increases. The porosity of the specimen with a 0° inclination angle is noticeably lower than that after one freeze-thaw time. The porosity increase of specimens with inclination angles of 45° and 60° is small. This is because the rise in the volume of frozen pore water leads to the expansion of pore volume, and small particles in the upper layer fall and fill the pores of large particles in the lower layer. Obviously, the filling rate of the specimen with a 0° inclination angle is greater than that of specimens with inclination angles of 45° and 60°. After ten freeze-thaw cycles, the porosity of each specimen continues to increase, indicating that the interface filling of the accumulation layer of specimens with various inclination angles is completed. The pore water of C and F tailings sand on the upper and lower layers of the accumulation interface is affected by freeze-thaw, resulting in an

increase in porosity. As the inclination angle of the interface increases, it becomes more difficult for upper-layer particles to fill lower-layer pores. Therefore, specimens with large inclination angles are more prone to particle torsion, sliding, and redistribution, and are more prone to strain softening. The porosity of specimens with inclination angles of 45° and 60° is between that of the C and F specimens, while the porosity of the specimen with a 0° inclination angle is greater than that of the C specimen. This shows that after five and ten freeze-thaw cycles, the particles of the specimen with a 0° inclination angle are more compact than those of the C specimen, and the occlusion and friction between particles are stronger than those of the C specimen. Therefore, under confining pressures of 200 kPa and 300 kPa, after five and ten freeze-thaw cycles, the strength of specimens with inclination angles of 45° and 60° is between that of the C and F specimens, while the strength of the specimen with a 0° inclination angle is higher than that of the C specimen.

As illustrated in Fig. 7, the peak area and porosity proportion of different pore size intervals of each specimen. From the Fig. 7, the peak area of C, F, 45°, and 60° specimens increases with the increase of number of freeze-thaw cycles, that is, the porosity increases with the rise of number of freeze-thaw cycles. The porosity of the 0° specimen shows periodic changes with the rise of number of freeze-thaw cycles. The crack pore size of the C specimen is obviously affected by freeze-thaw. As freeze-thaw cycles rise, the proportion of crack porosity rises significantly. The mesopore size interval of 0°, 45°, and 60° specimens shows an increasing trend with the rise of number of freeze-thaw cycles, and the proportion of peak area of mesopore size is not much different. The proportion of mesopore porosity of C and F specimens is obviously different from that of specimens with various inclination angles. The proportion of peak area of mesopore size of C specimen is relatively small, and the proportion of peak area of mesopore size of F specimen is relatively large. The proportion of peak area of small pore size of F specimen is smaller than that of C, 0°, 45°, and 60° specimens. Similarly, the proportion of peak area of large pore size of C specimen is greater than that of C, 0°, 45°, and 60° specimens. This shows that the pores of C specimen are mainly small and large pores, while the small, meso, and large pores of F specimen are evenly distributed. The pore distribution of 0°, 45°, and 60° specimens is between that of C and F specimens. Except for C and 0° specimens, the proportion of mesopore peak area of F, 45°, and 60° specimens shows a decreasing trend with the rise of freeze-thaw cycles. Combined with the rise of the proportion of large pore peak area of specimens, it shows that with the rise in number of freeze-thaw cycles, the mesopores in the specimens are interconnected to form large pores. While the proportion of small pore peak area of C specimen increases and the proportion of large pore peak area decreases, indicating that as the freeze-thaw cycles increase, large pores tend to decompose and break, forming smaller pores. And it further shows that under the action of freeze-thaw, the decomposition effect of large pores of tailings sand with particle size greater than 0.25 mm is obviously stronger than the interconnection of small pores. For

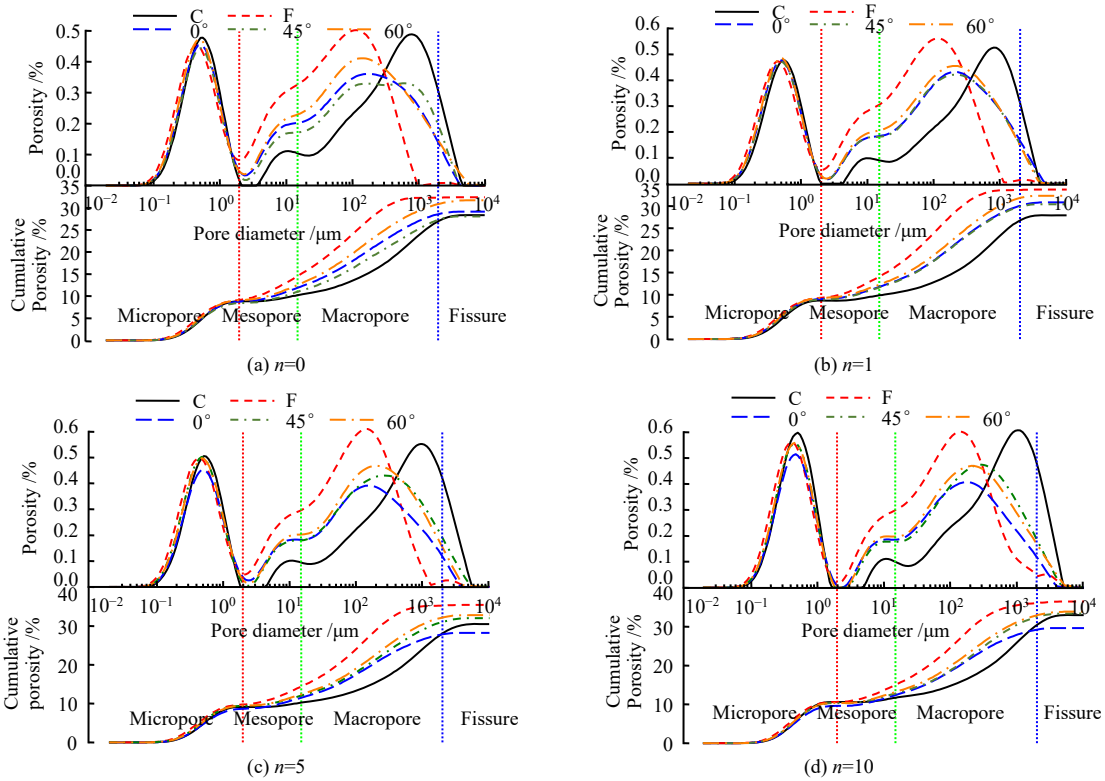


Fig. 6 Pore distribution of specimens with different dip angles

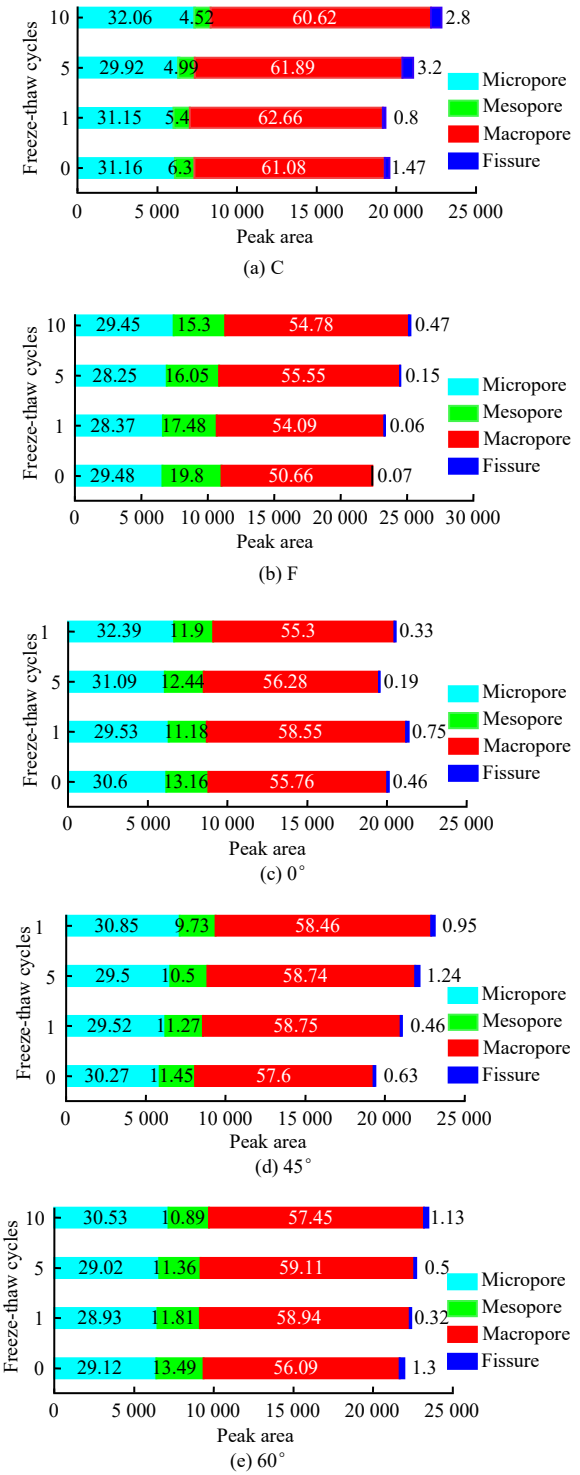


Fig. 7 Peak area and porosity ratio of different pore size intervals of each specimen

tailings sand with particle size less than 0.25 mm, the interconnection effect of small pores is greater than the decomposition of large pores. It is precisely because of the periodic changes of pores under the action of freeze-thaw that the cementation, occlusion and friction between tailings sand particles are greatly weakened, and then the strength is reduced[27-29].

4.2.2 Unfrozen water content

Previous studies have shown[27, 30]: The pore water of soil freezes in a low-temperature environment, but there is still some water attached to the particle surface in the form of bound water. In accordance with the study results of Thommes et al.[31] and combined with the test results of unfrozen water content of tailings sand, the following definitions are made: Relaxation time less than 3 ms is adsorbed water, relaxation time from 3 to 33 ms is capillary water, and relaxation time greater than 33 ms is free water.

Figure 8 shows the unfrozen water distribution characteristics of specimens with various inclination angles of the accumulation layer. Before freezing, most of the pore water in specimens with various inclination angles exists in the micropore, mesopore, and macropore intervals, and a small amount exists in fissures. The size of the adsorbed water peak area can be expressed as 60°>45°>0°. This is determined by the interface surface area of the accumulation layer of specimens with various inclination angles. A larger accumulation interface surface area means a closer contact between C and F particles. The spacing between particles is small and the contact surface is large. Therefore, the migration of film water on the particle surface is weakened, resulting in a larger adsorbed water peak area. And a larger adsorbed water peak

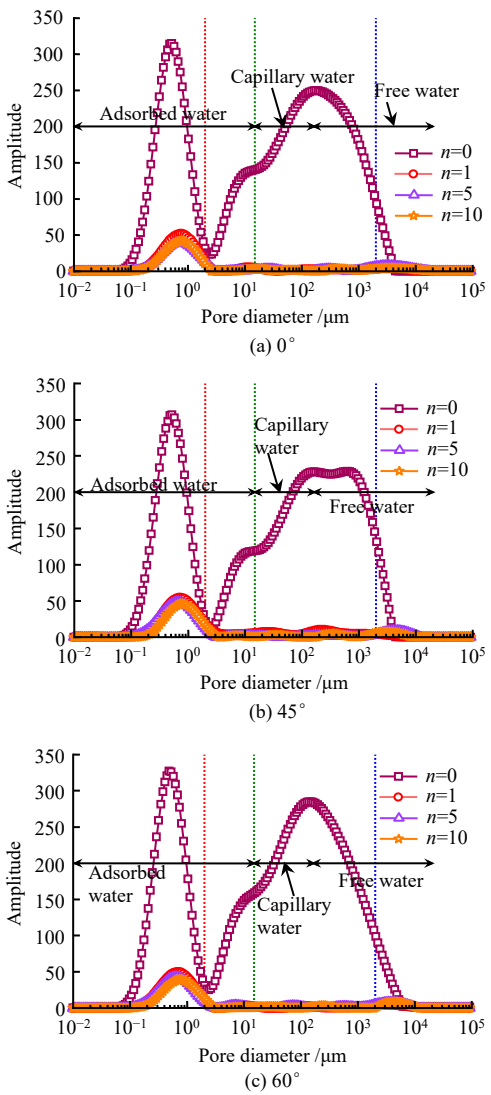


Fig. 8 Unfrozen water distribution of specimens with different interface inclination angles

area also means less pore water migration and weaker capillary action. Therefore, the relationship of capillary force can be expressed as 0°>45°>60°. This is also the reason why, in the triaxial test results mentioned above, with the increase in inclination angle, the rise in the shear strength of tailings sand specimens due to the first freeze-thaw time gradually decreases. The peaks of adsorbed water, capillary water, and free water of the 60° specimen are higher than those of 0° and 45°. This paper analyzes that the inclination angle of the 60° interface is large and the slope of the accumulation layer interface is relatively steep. Therefore, vertical migration of moisture in tailings sand between different particle sizes may occur, that is, moisture is not transferred through the accumulation interface.

Figure 9 shows the proportion of each moisture content and the unfrozen water moisture content of specimens with various inclination angles. From the Fig. 9, the proportions of adsorbed water, capillary water, and free water of specimens with inclination angles of 0°, 45°, and 60° show periodic changes. The

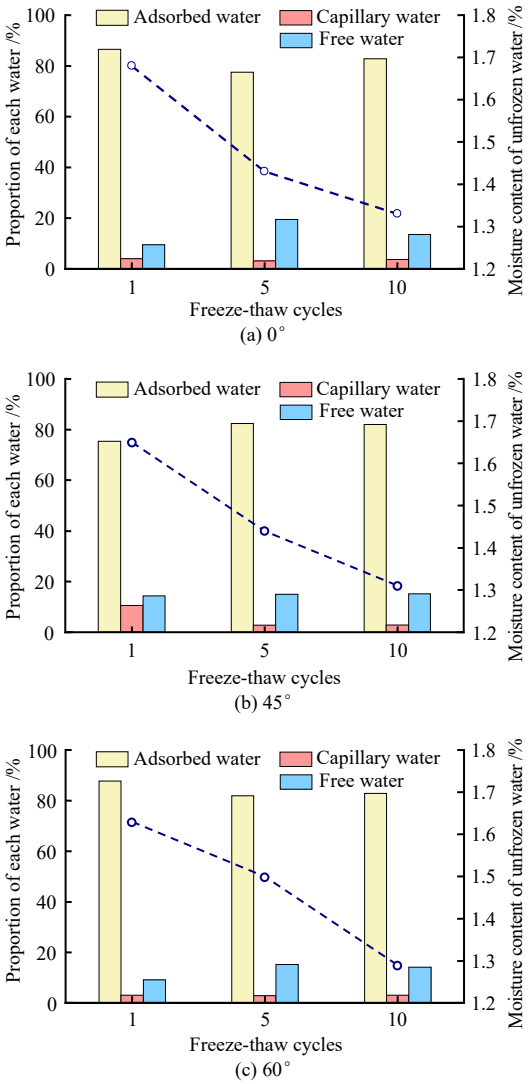


Fig. 9 Proportion of each moisture content and moisture content of unfrozen water of specimens with different inclination angles

adsorbed water and free water of each specimen show opposite change trends. This is because during the freezing process, the free water in large pores preferentially forms nucleation sites, and the water in small pores migrates to the freezing front due to the action of vapor flow and capillary force[32-34]. Therefore, after freezing, the adsorbed water decreases and the free water increases. The melting process is the opposite. Due to the water potential difference, the free water in the pores migrates, and some of the free water is transformed back into capillary water and adsorbed water. And the proportions of adsorbed water, capillary water, and free water of specimens with various inclination angles show periodic changes. This paper analyzes that the freeze-thaw cycle leads to the "migration and accumulation" phenomenon of pore water in specimens. That is, during the freezing process, most of the adsorbed water and capillary water are converted into free water. During the melting process, a small amount of free water is transformed back into adsorbed water and capillary water. The increase in the accumulation of free water leads to an increase in the volume expansion of pores due to the water-ice phase change and an increase in porosity. After melting, the pores are partially restored, and small particles enter the larger pore interval for filling, providing a basis for the migration of film water and capillary water. Therefore, the interface inclination angle can greatly shorten the "migration and accumulation" cycle. The presence of "migration and accumulation" of pore water significantly increases the expansion of pore space in iron tailings sand during the freezing process. When the ice crystals in the pores melt, the large pores collapse and split into smaller ones. This cyclic damage to the pore structure reduces the friction and interlocking forces between tailings particles, leading to a substantial decline in bearing capacity and severely undermining the structural stability of tailings deposits.

5 Mechanism of strength degradation

Since there is less water migration in the large pores of the specimen during the freezing process, it is assumed that the water in the large pores of the specimen freezes and expands in situ. As shown in Fig. 10, before freezing, there are interactions such as friction and cohesion between the representative elementary volume (REV) particles of tailings sand. During the freezing process, the pore water phase changes into ice and expands in volume, resulting in a reduction in the contact area between particles. The specific analysis is as follows:

Before freezing:

Terzaghi believed that the material reaches the yield strength of the material at the protruding contact points, that is:

$$A_{\mathrm{c}}=\frac{N}{\sigma_{\mathrm{y}}} \tag{3}$$

On the contact area A_{c} of the yield zone, if the shear

strength is τ_m, then the shear load T is:

$$T = A_c \tau_m \tag{4}$$

The friction coefficient μ is:

$$\mu = \frac{\tau_m}{\sigma_y} \tag{5}$$

Since the particle surface is not smooth and is covered by an adsorption film, the actual contact area between particles is greatly reduced, that is:

$$T = A_c[\delta\tau_m + (1-\delta)\tau_c] \tag{6}$$

where N is the overlying load; σ_y is the yield strength of the material; δ is the ratio of the actual contact area between particles to the total contact area; and τ_m and τ_c are the shear strengths between particles and between adsorption films, respectively.

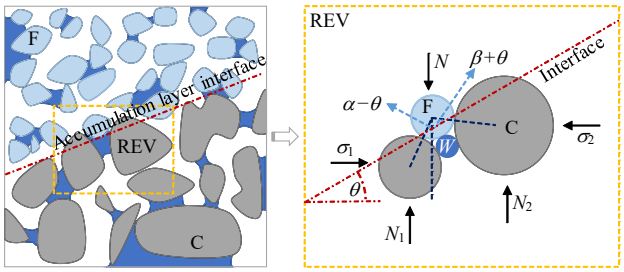


Fig. 10 Layered structure tailings particle distribution diagram

As mentioned above, during the freezing process of the tailings sand specimen, the volume expands, and some pores collapse after freezing. After freezing, the water content and pore volume of the water-containing pores increase. Existing studies have shown[35-36] that the phase change of soil pore water into ice causes the volume to expand and the pores to increase, and the volume expansion rate is about 9%. Assuming that the shapes of tailings sand particles, pores, and pore water are spherical, then the relationship between the radii r_w and r_{th} of the water-containing pores before and after freeze-thaw can be expressed as:

$$r_{th} = 1.03 r_w \tag{7}$$

Increment of water-containing pore radius Δr is

$$\Delta r = r_{th} - r_w = 0.03 r_w \tag{8}$$

The horizontal projection of the pore radius increment Δl is

$$\Delta l = \Delta r \cos\theta = 0.03 r_w \cos\theta \tag{9}$$

where θ is the inclination angle of the interlayer interface.

Affected by the expansion force, the cohesion between particles decreases, the cementation effect decreases, the particle spacing increases, and the contact surface decreases. Therefore, the shear load T of tailings sand after freezing decreases[16].

The overlying load N on the F tailings sand can be expressed as

$$\left.\begin{aligned} N\cos(\alpha-\theta) &= \sqrt{\sigma_1^2 + N_1^2} \\ N\cos(\beta+\theta) &= \sqrt{\sigma_2^2 + N_2^2} \end{aligned}\right\} \tag{10}$$

where α is the angle between the left coarse particle and the upper fine particle in Fig.10; β is the angle between the right coarse particle and the upper fine particle in Fig.10; σ_1 and N_1 are the horizontal and vertical supporting forces acting on the left coarse particle respectively; and σ_2 and N_2 are the horizontal and vertical supporting forces acting on the right coarse particle respectively.

As can be seen from Eq. (10), as the inclination angle of the interface increases, $\cos(\alpha-\theta)$ gradually increases, and the overlying load is directly borne by the particles in the lower layer, that is:

$$N = N_1 \tag{11}$$

Combining Eqs (6), (9)−(11), it can be noted that as the inclination angle of the interface increases, the horizontal projection of the increment of water-containing pores gradually decreases, and the horizontal component of the overlying load of small-sized tailings sand decreases. Therefore, the larger the inclination angle of the interface, the more difficult it is for small-sized tailings sand to fill the lower layer of large-sized tailings sand.

Under the influence of freeze-thaw cycles, tailings sand will undergo a periodic compaction process. Tailings particles show the characteristics of compression, torsion, sliding and redistribution. And the more number of freeze-thaw cycles there are, the more compaction stages there are, and the more times of particle redistribution there are. The effective stress between tailings sand particles decreases, and the torsion and sliding phenomena become more intense. When the pore water of tailings sand freezes, the large pores will experience pore collapse and fragmentation due to the influence of water-ice phase change. This will reduce the cementation between particles to a certain extent, leading to the degradation of the sand body's accumulation structure and the reduction of strength. Liu et al.[7] research shows that the destruction of cementation leads to the transformation of the stress-strain relationship and the decline of strength of tailings sand after freeze-thaw cycles.

Alshibli et al.[37] research demonstrates that the soil has the highest void ratio at the shear failure part. The nuclear magnetic resonance results of this paper show that after the action of freeze-thaw cycles, as the inclination angle of the accumulation layer increases, the porosity of the interface of the specimen accumulation layer increases. Therefore, as the inclination angle of the accumulation layer rises, the shear strength of tailings sand gradually decreases, which is consistent with the conclusion of Chen et al.[2] And the transverse fracture failure mode of the tailings sand specimen in this paper can be explained as follows: The porosity of F tailings sand particles is higher than that of the accumulation layer interface and C tailings sand, and the shape of F tailings sand particles is more regular and the surface roughness is lower than that of C tailings sand. Therefore, F tailings sand particles are more prone to movement and torsion, which is in line with the observation of Higo et al.[32] and others that

there is greater particle movement and rotation in the shear band of sand.

6 Conclusions

Taking macroscopic and microscopic perspectives as entry points, this paper focuses on analyzing the mechanical properties and pore evolution laws of the heterogeneous structure of tailings ponds under the action of freeze-thaw cycles. In accordance with the results of triaxial compression tests and nuclear magnetic resonance tests, the following conclusions are obtained:

(1) Under the action of freeze-thaw, the shear strength of the heterogeneous structure of tailings sand is lower than that of C tailings sand. And with the increase in freeze-thaw cycles, the strength reduction is significant. Under low confining pressure, as the inclination angle of the accumulation layer increases, it becomes more difficult for the upper layer particles to fill the lower layer pores. Specimens with large inclination angles are more prone to particle torsion, sliding, and redistribution, and are more likely to exhibit strain softening.

(2) The enhancement effect of initial freeze-thaw on the shear strength of tailings sand can be attributed to the increase in the internal friction angle. The combined action of the volume expansion of pore water phase change during freezing and the capillary force of pore water migration during freeze-thaw causes the torsion, movement, and redistribution of tailings sand particles, thereby promoting an increase in the internal friction angle.

(3) Under the influence of freeze-thaw cycles, the deformation modes of C, F, and specimens with various inclination angles can be summarized as: dilation, coexistence of dilation and contraction. The failure modes are transverse fracture. The shear deformation mode of C tailings sand is dilation. The shear deformation mode of F tailings sand and tailings sand with various inclination angles is the coexistence of shear and contraction. The failure mode of specimens with various inclination angles is transverse fracture.

(4) Under the influence of freeze-thaw cycles, there are two effects on the pores of tailings sand: decomposition and fragmentation of large pores to form smaller pores, and the connection of small pores to form large pores. For tailings sand with a particle size greater than 0.25 mm, the decomposition effect of large pores is stronger than the interconnection of small pores. For tailings sand with a particle size less than 0.25 mm, the interconnection effect of small pores is greater than the decomposition of large pores. It is the periodic change of pores that leads to the reduction of the strength of tailings sand.

(5) Freeze-thaw cycles lead to the "migration and accumulation" effect of pore water in tailings sand specimens, and the heterogeneous structure can greatly shorten the "migration and accumulation" cycle, showing more intense phenomena of small pore connection and large collapse.

Reference

[1] RICO M, BENITO G, SALGUEIRO A R, et al. Reported tailings dam failures: a review of the European incidents in the worldwide context[J]. Journal of Hazardous Materials, 2008, 152(2): 846-852.

[2] CHEN Q L, ZHANG C, YANG C H, et al. Strength and deformation of tailings with fine-grained interlayers[J]. Engineering Geology, 2019, 256: 110-120.

[3] COIMBRA K T O, ALCÂNTARA E, DE SOUZA FILHO C R. An assessment of natural and manmade hazard effects on the underwater light field of the Doce River continental shelf[J]. Science of the Total Environment, 2019, 685: 1087-1096.

[4] FRANCINI-FILHO R B, CORDEIRO M C, OMACHI C Y, et al. Remote sensing, isotopic composition and metagenomics analyses revealed Doce River ore plume reached the southern Abrolhos Bank Reefs[J]. Science of the Total Environment, 2019, 697: 134038.

[5] ROTTA L H S, ALCANTARA E, PARK E, et al. The 2019 Brumadinho tailings dam collapse: possible cause and impacts of the worst human and environmental disaster in Brazil[J]. International Journal of Applied Earth Observation and Geoinformation, 2020, 90: 102119.

[6] YIN G Z, LI G Z, WEI Z A, et al. Stability analysis of a copper tailings dam via laboratory model tests: a Chinese case study[J]. Minerals Engineering, 2011, 24(2): 122-130.

[7] LIU Y N, HUANG R Q, LIU E L, et al. Mechanical behaviour and constitutive model of tailing soils subjected to freeze- thaw cycles[J]. European Journal of Environmental and Civil Engineering, 2021, 25(4): 673-695.

[8] ZANDARÍN M T, OLDECOP L A, RODRÍGUEZ R, et al. The role of capillary water in the stability of tailing dams[J]. Engineering Geology, 2009, 105(1-2): 108-118.

[9] LIU Y N, LIU E L, YIN Z Y. Constitutive model for tailing soils subjected to freeze–thaw cycles based on meso-mechanics and homogenization theory[J]. Acta Geotechnica, 2020, 15(9): 2433-2450.

[10] LIU Y N, LIU E L. Study on cyclically dynamic behavior of tailing soil exposed to freeze-thaw cycles[J]. Cold Regions Science and Technology, 2020, 171: 102984.

[11] YANG Y H, WEI Z A, YIN G Z, et al. Uniaxial compression test of frozen tailings[J]. Cold Regions Science and Technology, 2016, 129: 60-68.

[12] WEI C, APEL D B, ZHANG Y. Shear behavior of ultrafine magnetite tailings subjected to freeze-thaw cycles[J]. International Journal of Mining Science and Technology, 2019, 29(4): 609-616.

[13] LI C J, JIN J X, WU P F, et al. Effect of freeze-thaw cycles on shear strength of tailings and prediction by grey model[J]. Minerals, 2022, 12(9): 1125.

[14] YANG X L, YAN R M. Collapse mechanism for deep

tunnel subjected to seepage force in layered soils[J]. Geomechanics & Engineering, 2015, 8(5): 741-756.

[15] SAMANTA M, PUNETHA P, SHARMA M. Effect of roughness on interface shear behavior of sand with steel and concrete surface[J]. Geomechanics & Engineering, 2018, 14(4): 387-398.

[16] ZHANG Q G, YIN G Z, WEI Z A, et al. An experimental study of the mechanical features of layered structures in dam tailings from macroscopic and microscopic points of view[J]. Engineering Geology, 2015, 195: 142-154.

[17] TIAN S, HE Y, BAI R Y, et al. Experimental study on consolidation and strength properties of tailings with different particle size distribution characteristics[J]. Natural Hazards, 2022, 114(3): 3683-3699.

[18] ZHANG H, LI Q M, GENG C, et al. Study of the static mechanical properties of tailings under the influence of multiple lens types[J]. Mechanics of Advanced Materials and Structures, 2025, 32(7): 1458-1466.

[19] Ministry of Housing and Urban-Rural Development of the People's Republic of China. GB 50863－2013 Code for design of tailings facilities[S]. Beijing: China Planning Press, 2013.

[20] ZHAO T B, GUO W Y, LU C P, et al. Failure characteristics of combined coal-rock with different interfacial angles[J]. Geomechanics & Engineering, 2016, 11(3): 345-359.

[21] Ministry of Housing and Urban-rural Development of the People's Republic of China. GB/T 50123－2019 Standard for geotechnical testing method[S]. Beijing: China Planning Press, 2019.

[22] CABRERA S C M, BRYAN J, KOMISHKE B, et al. Study of the settling characteristics of tailings using nuclear magnetic resonance technique[J]. International Journal of Mining, Reclamation and Environment, 2009, 23(1): 33-50.

[23] BABAK P, LI F, CABRERA S M, et al. Laboratory monitoring approaches for tailings settling and evaluation of flocculant and coagulant treatments[J]. The Canadian Journal of Chemical Engineering, 2021, 99(12): 2702-2712.

[24] LI Tian-guo, KONG Ling-wei, WANG Jun-tao, et al. Trimodal pore structure evolution of expansive soil in seasonal frozen area based on nuclear magnetic resonance[J]. Rock and Soil Mechanics, 2021, 42(10): 2741-2754.

[25] FAN W, YANG P, YANG Z J. Freeze-thaw impact on macropore structure of clay by 3D X-ray computed tomography[J]. Engineering Geology, 2021, 280: 105921.

[26] WANG En-liang, LIU Cheng-qian, LIU Xing-chao, et al. Study on pore and shear strength of expansive soil based on nuclear magnetic resonance technology under freeze-thaw conditions[J]. Journal of Glaciology and Geocryology, 2024, 46(3): 919-929.

[27] XU J, LI Y F, LAN W, et al. Shear strength and damage mechanism of saline intact loess after freeze-thaw cycling[J]. Cold Regions Science and Technology, 2019, 164: 102779.

[28] GAO Z, HU X, LI X Y, et al. Effects of freeze-thaw cycles on soil macropores and its implications on formation of hummocks in alpine meadows in the Qinghai Lake watershed, northeastern Qinghai-Tibet Plateau[J]. Journal of Soils and Sediments, 2021, 21(1): 245-256.

[29] MIRANDA-VELEZ J F, LEUTHER F, KOEHNE J M, et al. Effects of freeze-thaw cycles on soil structure under different tillage and plant cover management practices[J]. Soil and Tillage Research, 2023, 225: 105540.

[30] YAN Chang-gen, WANG Ting, JIA Hai-liang, et al. Effect of unfrozen water content on shear strength of unsaturated silt during freezing-thawing process[J]. Chinese Journal of Rock Mechanics and Engineering, 2019, 38(6): 1252-1260.

[31] THOMMES M, KANEKO K, NEIMARK A V, et al. Physisorption of gases, with special reference to the evaluation of surface area and pore size distribution (IUPAC Technical Report)[J]. Pure and Applied Chemistry, 2015, 87(9-10): 1051-1069.

[32] HIGO Y, OKA F, KIMOTO S, et al. Study of strain localization and microstructural changes in partially saturated sand during triaxial tests using microfocus X-ray CT[J]. Soils and Foundations, 2011, 51(1): 95-111.

[33] ZHANG S, TENG J D, HE Z Y, et al. Canopy effect caused by vapour transfer in covered freezing soils[J]. Géotechnique, 2016, 66(11): 927-940.

[34] TENG J, SHAN F, HE Z, et al. Experimental study of ice accumulation in unsaturated clean sand[J]. Géotechnique, 2019, 69(3): 251-259.

[35] ZHANG Z, MA W, FENG W J, et al. Reconstruction of soil particle composition during freeze-thaw cycling: a review[J]. Pedosphere, 2016, 26(2): 167-179.

[36] LIU B, MA R M, FAN H M. Evaluation of the impact of freeze-thaw cycles on pore structure characteristics of black soil using X-ray computed tomography[J]. Soil and Tillage Research, 2021, 206: 104810.

[37] ALSHIBLI K A, HASAN A. Spatial variation of void ratio and shear band thickness in sand using X-ray computed tomography[J]. Géotechnique, 2008, 58(4): 249-257.